Laboratory Experiments on the Transition of Wind-Driven Water Surface

Daisuke MIYAZAKI[*1] Yuji SUGIHARA[*2,†] Yoshihiro NAKAMURA[*3]
Michio SANJOU[*4] and Takaaki OKAMOTO[*4]
[†]E-mail of corresponding author: sugihara@esst.kyushu-u.ac.jp

In order to investigate the transition process of the wind-driven water surface, laboratory experiments were made in a wind-water tunnel with a pipe for the circulation of water. In addition to visual observation of the water surface, measurements of the wind speed, the wind wave and the drift current in water were carried out in the present experiments. We focused on the relationship between the transition process and some wind-wave parameters, and examined if what kind of parameter is effective for identifying the wave breaking. The behavior of the drift current velocity in water was found to be varied by the occurrence of the micro wave breaking on the surface. It was concluded that the drift current velocity gives an important aspect of the momentum transfer across the water surface, so that it becomes a significant index to describe the transition process of the wind-driven water surface.

Key words: *Wind wave, Wave breaking, Drift current, Transition process, Friction Velocity, Wind-water tunnel experiment*

1. Introduction

The exchange mechanism of the momentum or gases across the ocean surface is governed by turbulence dynamics coupled to the wave breaking phenomenon. Such a dynamics varies obviously depending on the aspect of the wind-driven water surface, corresponding to wind velocity and wave field conditions. The transition of the water surface with increase of the wind velocity is mostly as follows: the water surface first shifts from the complete smooth surface to the capillary wave surface. In the next stage, the gravitational wind-driven waves occur on the surface, and such waves reach the wave breaking when exceeding a certain critical condition. The surface with violently-breaking waves becomes the completely rough surface. The transition process is complexly intertwined with the momentum transfer between the atmosphere and the ocean, and it is regarded as a certain critical phenomenon for the occurrence of the wave breaking. Thus, it is important to find out dimensionless parameters to identify the transitional process, especially the wave breaking.

Many studies have been made to investigate the transition process of the wind-driven water surface. Developing wind-waves trend to be equilibrated locally with wind[1], [2]. Such wave fields are well known to satisfy Toba's 3/2-power law, which is a similarity law covering a wide range of wind waves. Toba and Koga[3] proposed a parameter suitable for expressing the occurrence of the wave breaking. It is called the windsea Reynolds number[4], and defined by the following relation:

$$ R_B = \frac{u_*^2}{\omega_p \nu_a}, \qquad (1) $$

where u_* is the friction velocity on airside, ν_a the kinematic viscosity of air, and ω_p the spectral-peak wave angular frequency. In a range of $R_B > 10^3$, the wind-driven water surface becomes violently-breaking waves with the generations of bubbles and water spray. Also, Mitsuyasu[5] found that the aspect of the wind-driven water surface varies around $u_* =$

---

*1 ING SHOJI, Co., Ltd.
*2 Department of Earth System Science and Technology
*3 Department of Earth System Science and Technology, Graduate Student
*4 Department of Civil and Earth Resources Engineering, Kyoto University

0.2m/s, and that the relations of the mean wind speed and the wave spectrum with the friction velocity vary around $u_* = 0.2$m/s. The value corresponds approximately to the mean wind speed of approximately 8m/s, which is well known to that at the occurrence of the whitecaps on the ocean surface.

The purpose of this study is to examine the transition process of the wind-driven water surface. Laboratory experiments were made in a wind-water tunnel with a pipe for the circulation of water. In addition to visual observation of the water surface, measurements of the wind speed, the wind wave and the drift current in water were carried out in the experiments. We investigated the relationship between the transition process and some wind-wave parameters, and examined the validities of the parameters for identifying the wave breaking.

2. Experimental Procedure

Laboratory experiments were performed in a wind-water tunnel with a pipe for the circulation of water, at the Graduate School of Engineering, Kyoto University. Figure 1 shows a schematic diagram of the experimental apparatus. The tank was 16m

long, 0.4 m wide, and 0.50 m deep. The wind-driven water flow can circulate through the pipe, so that no return flow appears in the water tank. Tap water was used in the experiments, and the water depth was kept at 0.25 m in all cases. Measurements were carried out at the fetch of 8.0 m, which denotes the distance taken leeward from the upwind edge in the tunnel. The vertical profile of the wind speed was measured by using a hot-wire anemometer. In addition, the displacement of the water surface was measured using a capacitance wave gage. The significant wave height H_s, the spectral-peak wave period T_p, and the spectral-peak angular frequency ω_p were calculated from the data of the surface displacement. The flow rate of the drift current in water driven by the wind stress was measured using an electromagnetic flowmeter attached to the circular pipe.

Experimental parameters are summarized in Table 1, where U_r is a reference wind speed at the fetch of the wind-water tunnel, and u_* and u_{*w} are the friction velocities on airside and waterside, respectively. Also, U_{10} indicates the mean wind speed at the height of 10 m from the water surface. The value has been calculated by fitting the logarithmic law to the profile of wind speed near the water
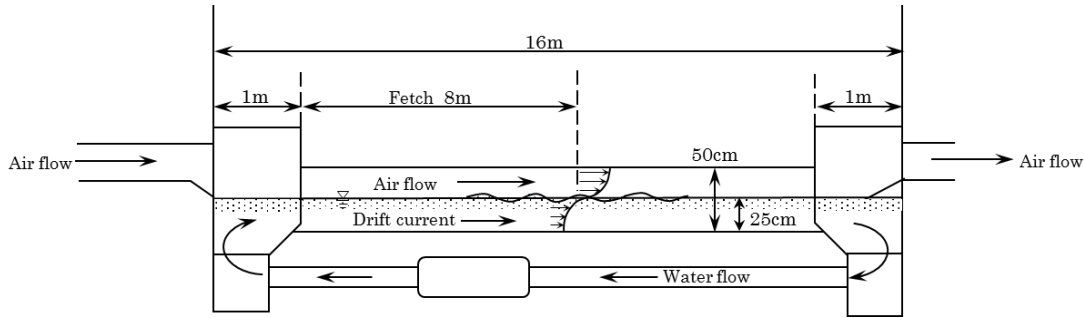

Fig. 1 Experimental apparatus

Table 1 Experimental parameters

case	U_r(m/s)	u_*(m/s)	u_{*w}(m/s)	U_{10}(m/s)	H_s(m)	T_p(s)	Q(l/s)	Surface aspect
1	1.75	0.017	5.92E−04	1.75	9.39E−04	−	0.19	Complete smooth surface
2	2.31	0.023	7.91E−04	2.48	2.71E−03	−	0.32	Capillary wave
3	2.88	0.035	1.20E−03	2.73	5.36E−03	−	0.51	″
4	3.44	0.040	1.38E−03	3.39	1.01E−02	0.298	0.80	Gravitational wind−wave
5	4.04	0.067	2.32E−03	4.29	1.42E−02	0.312	0.96	″
6	4.58	0.081	2.78E−03	5.38	1.81E−02	0.377	1.23	Micro wave breaking [MB]
7	5.14	0.140	4.81E−03	6.87	2.19E−02	0.388	1.48	″
8	5.70	0.153	5.27E−03	7.32	2.69E−02	0.400	1.69	″
9	6.31	0.223	7.67E−03	8.89	2.91E−02	0.427	2.00	Wave breaking [B]
10	6.89	0.407	1.40E−02	12.6	3.39E−02	0.427	2.29	
11	7.39	0.520	1.79E−02	13.8	3.68E−02	0.441	2.63	″
12	7.83	0.584	2.01E−02	14.4	4.05E−02	0.457	2.96	″
13	8.31	0.598	2.06E−02	15.9	4.67E−02	0.474	3.32	Wave breaking with bubble [BB]
14	8.67	0.959	3.30E−02	21.6	4.98E−02	0.492	3.69	″
15	9.06	1.333	4.58E−02	26.6	5.45E−02	0.492	4.03	″
16	9.44	1.401	4.81E−02	27.6	5.87E−02	0.512	4.37	″
17	9.50	1.712	5.88E−02	31.0	6.23E−02	0.533	4.65	″
18	9.83	1.757	6.04E−02	31.6	6.75E−02	0.582	4.86	″

surface. We should note that the value of u_{*w} has been obtained from the following relation:

$$\rho_a u_*^2 = \rho_w u_{*w}^2 \qquad (1)$$

with ρ_a and ρ_w being the densities of air and water, respectively. The above relation means the continuity of the momentum transfer across the water surface. The values of ω_p in the cases of 1 to 3 couldn't be obtained from the spectra. Table 1 also gives the aspects of the wind-driven water surface identfied by visual observation. In this study, the patterns of the wave breaking were classified on the basis of the scale of the wind waves. The slightly-breaking waves due to the instability of the wave train are called the micro wave breaking, which is expressed by the symbol of **MB**（Micro Breaking）. In addition, the wave breaking with no clearly visible bubbles is expressed by **B**（Breaking）, and the symbol of **BB**（Breaking with Bubble）gives the violent wave-breaking with the generation of visible bubbles. It should be noted that in wind-water tunnel experiments, the sale of the wind-driven wave must be limited in the width of the wind-water tunnel, so that properties of the wind waves may be different between laboratory water surfaces and actual ocean surfaces at high wind speeds.

3. Results and Discussion

3.1 Transition of Wind-Driven Water Surface

Figures 3 (*a*)-(*f*) show typical patterns of the wind-driven water surfaces photographed under the conditions of various wind speeds, where the shutter speed of camera was 100 fps in a range of $U_r < 6.31$ m/s, and otherwise the speed was 125 fps. Features of the wind-driven water surface observed at each wind speed, i.e., the transition process, are as follows:

(*a*) $U_r = 2.31$ m/s（$U_{10} = 2.48$ m/s, $u_* = 0.023$ m/s）: capillary wave occurs on the surface.

(*b*) $U_r = 3.44$ m/s（$U_{10} = 3.39$ m/s, $u_* = 0.040$ m/s）: Gravitational wind-wave is observed.

(*c*) $U_r = 4.58$ m/s（$U_{10} = 5.38$ m/s, $u_* = 0.081$ m/s）: the instability of wave train occurs, and the micro breaking of wave crest is observed [**MB**].

(*d*) $U_r = 6.31$ m/s（$U_{10} = 8.89$ m/s, $u_* = 0.223$ m/s）: definitely breaking waves are obviously shown, and the water surface may become incomplete rough one, but the bubbles in the water are indistinct [**B**].

(*a*) $U_r = 2.31$ m/s（$U_{10} = 2.48$ m/s, $u_* = 0.023$ m/s）

(*d*) $U_r = 6.31$ m/s（$U_{10} = 8.89$ m/s, $u_* = 0.223$ m/s）[**B**]

(*b*) $U_r = 3.44$ m/s（$U_{10} = 3.39$ m/s, $u_* = 0.040$ m/s）

(*e*) $U_r = 8.31$ m/s（$U_{10} = 15.9$ m/s, $u_* = 0.598$ m/s）[**BB**]

(*c*) $U_r = 4.58$ m/s（$U_{10} = 5.38$ m/s, $u_* = 0.081$ m/s）[**MB**]

(*f*) $U_r = 9.44$ m/s（$U_{10} = 27.6$ m/s, $u_* = 1.401$ m/s）

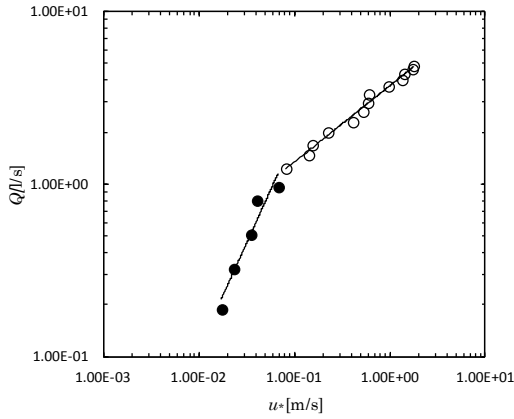**Fig. 2** Visualized transition process of wind-driven water surface
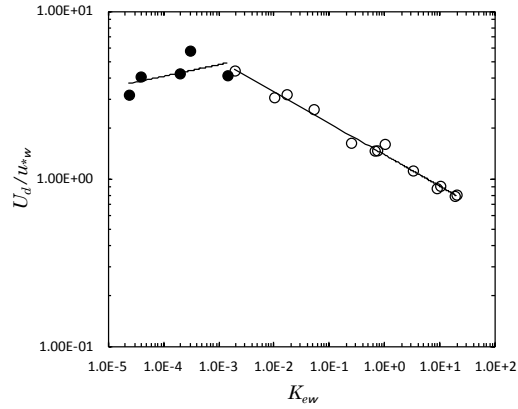
Fig. 3 Relation between Q and u_*
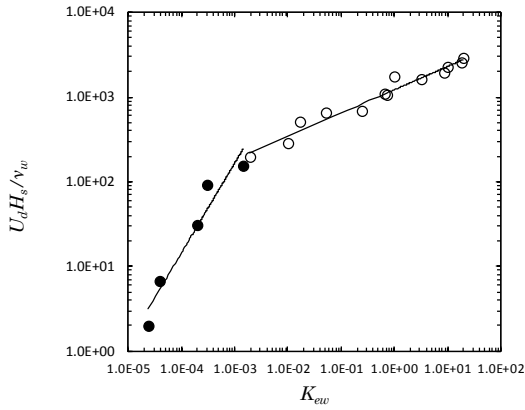

Fig. 4 Relation between U_d/u_{*w} and Ke_w

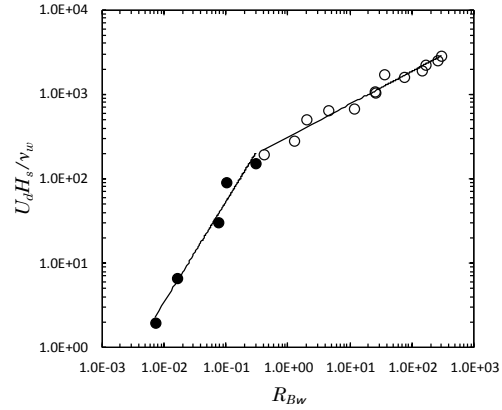**Fig. 5** Relation between U_dH_s/ν_w and Ke_w

Fig. 6 Relation between U_dH_s/ν_w and R_{Bw}

(*e*) $U_r = 8.31$ m/s （$U_{10} = 15.9$ m/s, $u_* = 0.598$ m/s） : the wave breaking with bubbles occurs [**BB**].

(*f*) $U_r = 9.44$ m/s （$U_{10} = 27.6$ m/s, $u_* = 1.401$ m/s） : the water spray produced due to the wave breaking is observed.

The above process may show the typical aspects of the wind-driven water surface observed in laboratory experiments. In this study, the wind speed condition under which the micro wave breaking occurs, becomes approximately U_{10}=5m/s. In addition, the condition for definite wave-breaking may be below approximately $U_{10}=8$m/s. The friction velocity on airside for this value of U_{10} agrees approximately with 0.2 m/s, whose value is the critical friction velocity proposed by Mitsuyasu[5]. Large-scale wave breaking with the generation of bubbles may occur approximately at $U_{10}=15$m/s, which agrees with the windsea Reynolds number R_B of 1.7×10^3. This value corresponds to the

critical windsea Reynolds number of the order of 10^3, proposed by Koga and Toba[3]. Therefore, the validity of the transition of the wind-driven water surface in the present experiments may be supported by the results of previous studies. It should be noted that under high wind speed conditions, the accuracies of u_* and U_{10} decrease in the comparison with lower wind speed conditions because of the difficulty of the wind speed measurements close to the water surface and the influence of the water spray in air.

3.2 Relationship between Transition Process and Drift Current Velocity

Figure 3 shows the relation between the flow rate of the drift current Q and the friction velocity on airside u_*. Here, the two solid lines are drawn in the figure, and they denote the regression lines for the ranges before and behind approximately u_*=0.1m/s. It is seen from the figure that the gradients of the two lines vary definitely before and behind this

point. The value of $u_* = 0.1$m/s corresponds approximately to the condition that the micro wave breaking occurs on the water surface, as pointed out in the previous section. The wind stress acting on the water surface drives the wind waves and the drift current in water. In the range of relatively low wind speeds, the momentum of wind is considered to be transferred mainly to the waterside via the friction on the water surface. Thus, it is natural to consider that under such conditions, the momentum may be injected to drive the drift current in water, not to develop wind waves. After the generation of the wave breaking, the momentum transferred from wind may increase the momentum in the flow direction through the wave breaking process. In addition, eddy motions induced by the wave breaking should diffuse the turbulent energy near the water surface. The increase of the eddy viscosity via such a process promotes the air-water exchange process. Thus, the decrease of the gradient of Q due to the micro wave breaking may be understood that the momentum transferred from wind is used to develop the wave motions. The finding that the drift current varies at a certain critical condition relating to the wave breaking is very interesting from viewpoint of fluid dynamics.

The mean drift current velocity U_d was calculated by averaging the value of Q over the cross-section area of water flow. In Fig. 4, the values of U_d normalized by the friction velocity on waterside u_{*w} are plotted for the Keulegan number defined by

$$Kew = \frac{u_{*w}^3}{g\nu_w} \qquad (2)$$

where g and ν_w are the gravitational acceleration and the kinematic viscosity of water, respectively. The two solid lines are the regression lines before and behind the occurrence of the micro wave breaking. The critical Keulegan number for the micro wave breaking becomes approximately $Kew = 2.0 \times 10^{-3}$. This figure shows that before the critical number, the dimensionless drift current velocity increases slightly with Kew, whereas it decreases definitely with increase of Kew behind the critical value. Such a behavior of the drift current velocity supports the hypothesis that when generating the wave breaking, the momentum transfer to the wave development becomes larger compared to that transferred to the shear flow.

Figure 5 indicates the relation between U_dH_s/ν_w and Kew, where the parameter U_dH_s/ν_w can be interpreted as a certain Reynolds
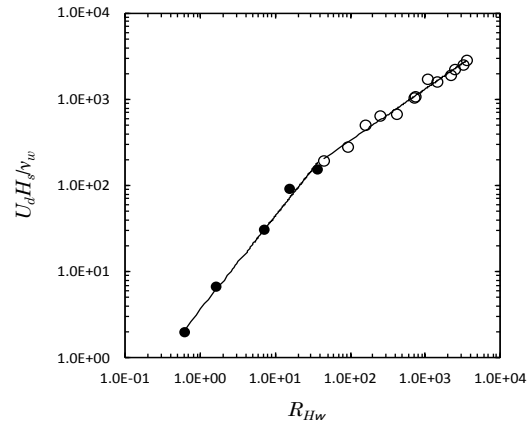

Fig. 7 Relation between U_dH_s/ν_w and R_{Hw}

number based on the drift current and the wave height. Across the critical value of the Keulegan number for the micro wave breaking, the gradient of U_dH_s/ν_w against Kew varies obviously. However, the other types of the wave breaking such as **B** and **BB** cannot be observed in this figure.

According to Koga and Toba[3] and Toba et al. [4], we consider the windsea Reynolds number R_{Bw}, defined by the friction velocity and the kinematic viscosity on waterside as follows:

$$R_{Bw} = \frac{u_{*w}^2}{\omega_p \nu_w} \qquad (3)$$

The relation of U_dH_s/ν_w with R_{Bw} is displayed in Fig. 6. We should note that the values of ω_p in the cases of 1 to 3 have been estimated conveniently from the values of H_s via Toba's 3/2-power law. The behavior of the experimental data on the space of these dimensionless parameters is found to be quantitatively similar to those in Fig. 5. We also should note that the critical value of R_{Bw} appears around approximately the order of 0.1. This suggests that it is suitable for the scaling to use the physical quantities on waterside. That may be because the phenomenon of the wave breaking appears on the surface of the water waves.

Figure 7 indicates the relation between U_dH_s/ν_w and R_{Hw}, where R_{Hw} is a windsea Reynolds number defined by

$$R_{Hw} = \frac{u_{*w}H_s}{\nu_w} \qquad (4)$$

This figure shows the gradient change around the micro wave breaking becomes quite smaller in comparison with Kew and R_{Bw}. The behavior can be expressed approximately

by a certain one regression curve. Therefore, the dimensionless parameter R_{Hw} may be insensitive to identify the critical condition of the micro wave breaking. Conversely, there is a possibility that R_{Hw} is a universal wind-wave parameter independent of the transition process such as the wave breaking.

4.   Summary and Conclusion

In this study, the transition process of the wind-driven water surface was investigated through the wind-water tunnel experiments. The visual observation of the water surface was made, and the wind speed, the wind wave and the drift current in water were measured under various wind speed conditions. We treated with the relationship between the transition process and some wind-wave parameters. The behavior of the drift current velocity in water was found to be varied by the occurrence of the micro wave breaking on the water surface. It was concluded that the drift current velocity gives an important aspect of the momentum transfer across the water surface, so that it becomes a significant index to describe the transition process of wind-driven water surface. We also demonstrated that the wind-wave parameters such as the Keulegan number and the windsea Reynolds number can express the critical condition of the micro wave breaking.

References

1) Toba, Y., Local balance in the air-sea boundary processes I. On the growth Processes of wind waves, *J. Oceanogr.*, 28, pp. 109–121, (1972).
2) Masuda, A., and T. Kusaba, On the local equilibrium of winds and wind-waves in relation to surface drag, *J. Oceanogr. Soc. Japan*, 43, pp. 28–36, (1987).
3) Toba, Y. and M. Koga, A parameter describing overall conditions of wave breaking, whitecapping, sea-spray production and wind stress, *Oceanic Whitecaps*, edited by E. C. Monahan and G. Mac Niocaoll, D. Reidel, pp. 37–46, (1986).
4) Toba, Y, S. Komori, Y. Suzuki and D. Zhao, Similarity and dissimilarity in air-sea momentum and CO_2 transfers: the nondimensional transfer coefficients in light of windsea Rynolds number, *Atomosphere-Ocean Interaction Volume 2, Ed. W. Perrie, WTT Press*, pp. 53-82., (2006).
5) Mitsuyasu, H., A note on a critical wind speed for air-sea boundary process, *J. Oceanogr*, 73, pp. 169–180, (2017).